ELEMENTAL ANALYSES OF HYPERVELOCITY MICROPARTICLE IMPACT SITES ON INTERPLANETARY DUST EXPERIMENT SENSOR SURFACES

C. G. Simon
Institute for Space Science and Technology
Gainesville, FL 32609

J.L. Hunter, D.P. Griffis, V. Misra, D.A. Ricks, J.J. Wortman
Analytical Instrumentation Facility, North Carolina State University
Raleigh, NC 27695

D.E. Brownlee,
Astronomy Department, University of Washington
Seattle, WA 98195

ABSTRACT

The Interplanetary Dust Experiment (IDE) had over 450 electrically active ultra-high purity metal-oxide-silicon impact detectors located on the six primary sides of the Long Duration Exposure Facility (LDEF). Hypervelocity microparticles (~0.2 to ~100 μm diameter) that struck the active sensors with enough energy to breakdown the 0.4 or 1.0 μm thick SiO_2 insulator layer separating the silicon base (the negative electrode), and the 1000Å thick surface layer of aluminum (the positive electrode) caused electrical discharges that were recorded for the first year of orbit. The high purity Al-SiO_2-Si substrates allowed detection of trace (ppm) amounts of hypervelocity impactor residues.

After sputtering through a layer of surface contamination, secondary ion mass spectrometry (SIMS) was used to create two-dimensional elemental ion intensity maps of microparticle impact sites on the IDE sensors. The element intensities in the central craters of the impacts were corrected for relative ion yields and instrumental conditions and then normalized to silicon. The results were used to classify the particles' origins as "manmade", "natural" or "indeterminate". The last classification resulted from the presence of too little impactor residue, analytical interference from high background contamination, the lack of information on silicon and aluminum residues, or a combination of these circumstances.

Several analytical "blank" discharges were induced on flight sensors by pressing down on the sensor surface with a pure silicon shard. Analyses of these blank discharges showed that the discharge energy blasts away the layer of surface contamination. Only Si and Al were detected inside the discharge zones, including the central craters, of these features.

Thus far a total of 79 randomly selected microparticle impact sites from the six primary sides of the LDEF have been analyzed: 36 from tray C-9 (Leading [ram], or East, side), 18 from tray C-3 (Trailing [wake], or West, side), 12 from tray B-12 (North side), 4 from tray D-6 (South side), 3 from tray H-11 (Space end), and 6 from tray G-10 (Earth end). Residue from manmade debris has been identified in craters on all trays. (Aluminum oxide particle residues were not detectable on the Al/Si substrates.)

These results were consistent with the IDE impact record which showed highly variable long term microparticle impact flux rates on the West, Space and Earth sides of the LDEF which could not be ascribed to astronomical variability of micrometeorite density. The IDE record also showed episodic bursts of microparticle impacts on the East, North and South sides of the satellite, denoting passage through orbital debris clouds or rings.

INTRODUCTION

The Interplanetary Dust Experiment (IDE) had approximately 450 high purity MOS type detectors mounted on the six primary sides of the stabilized spacecraft. The sensors were constructed from 2 inch diameter, 250 μm thick, boron-doped ultra high-purity silicon wafers covered with either a 0.4 or a 1.0 μm thick layer of thermally grown SiO_2 insulator, and coated with ~1000Å of high-purity aluminum. The location and identification of microparticle hypervelocity impacts on the formerly active detectors was facilitated by the presence of 50 μm wide "discharge zones" in the Al top layer surrounding each impact (see Figs. 1-3). It is also suspected that the negatively biased Si electrode surface exposed in the impact cratering event enhanced the collection efficiency of positive ions formed from impactor materials in the impact plasma.

The objective of the chemical analysis study is to empirically determine the manmade-to-natural microparticle population ratio of impactors that struck the LDEF satellite while in orbit. The study takes advantage of the purity of the IDE substrates and their location on all six primary sides of the satellite. Data from this study will be added to the growing pool of orbital hypervelocity impact site analyses produced from studies of the Solar Max, Palapa B and LDEF satellites.

EXPERIMENTAL

The detailed analysis protocol developed specifically for the IDE samples is described elsewhere (ref. 1). Optical microscopy and field-emission scanning electron microscopy (SEM) were used to locate and record the morphology of microparticle impact sites. Energy dispersive x-ray spectroscopy (EDS) and secondary ion mass spectrometry (SIMS) were used to look for and map the distributions of residual impactor debris in and around the impact craters. The presence and relative abundances of elements found in the craters were used to classify impactors as "manmade", "natural" or "indeterminate". Examples are presented in the following section.

EDS analyses of microparticle impact sites on the IDE sensor were limited in scope due to the concentrations of residue (~1%) required to produce detectable signals using EDS compared to the (ppm) concentrations needed to yield semi-quantitative results using the far more sensitive SIMS techniques. EDS and Auger electron spectroscopy (AES) were used to further analyze high concentration deposits of material (residues and contaminants) that were identified in and around impact sites with SIMS.

As previously described (ref. 1), all SIMS data was collected with a Cameca IMS 3F using $^{16}O^+$ or $^{16}O^-$ ion beams. The instrument was used in the ion microscope mode and data was recorded as two-dimensional elemental positive ion maps with lateral resolution of 1-2 μm. Pixel intensities were used to calculate relative element abundances. Briefly, the SIMS analytical protocol involves the following steps:

1.) Each impact site was first sputtered with the oxygen beam while monitoring the concentrations of C, Na and Mg in order to assure removal of the bulk of the surface contamination layer ubiquitous to LDEF.

2.) Next, an energy filtered bargraph type mass spectrum was recorded.

3.) Then, a dual channel-plate/ccd-digital-camera detector system was used to record high resolution ($M/\Delta M$= 3,000-4,000) elemental positive ion maps for C, O, Na, Mg, Si, Al, K, Ca, Ti, Cr, Fe, Ni, Cu, Zn, Ag and Au, and molecular ion maps for $^{56}Si_2$ and $^{58}Si_2$. (Images were not recorded if there were less than ~4 ion counts/min at the observed mass.)

4.) If there was enough of the IDE sensor's 1000Å Al top layer remaining around the impact site to prevent sample charging, negative elemental ion maps were recorded for H, C, O, F, Si, Al, S, Cl and Au.

Analysis of impacts on Ge witness plates flown on tray B-12 as part of the IDE experiment has been suspended. A summary of the work done to date on two of the Ge wafers, including crater counts and dimensions, description of contamination problems, and SIMS and/or EDS analyses for 13 impact sites, was presented in the LDEF First Post-Retrieval Symposium Proceedings (ref. 1). Contamination feature counts, crater counts, and representative photographs were recorded for all other witness plates mounted on LDEF tray B-12 along with the Ge plates. These included three 1" square Si plates from Washington University (Expt AO187) and ten zirconia, quartz and sapphire plates from NCSU with a total surface area of ~4 in^2. Results from these other witness plates showed clearly that the Ge witness plates were exposed to a major pre-flight contamination event.

The IDE Microparticle Impact Sample Set

The sample set for the study was composed of impacts selected from the 215 IDE sensors that have 1.0 μm thick insulator layers. These sensors were selected over the ones with thinner insulators because their electronically sturdier structure resulted in the majority of them remaining active for the entire 5.77 year LDEF orbital lifetime. Thus, no time bias was introduced into the sample set. The only selection criterion used was size. Impact craters with spall dimensions less than 30 μm were the focus of the study, but a few larger craters were also analyzed.

In order to gather data from a statistically significant fraction of this microparticle impact sample set, the total number of these impacts on each sensor group located on the six primary sides of LDEF was determined. Then, using 10% statistics, the total number of analyses required to achieve a significant fraction was calculated. This technique assumes that the statistics of a randomly selected group of 10% of the samples in a large, random sample set will, to first order, represent the statistics of the entire sample set.

The microparticle impact sample sets on the West, Space and Earth end IDE sensors are comprised of 290, 600 and 330 impact sites, respectively. Analyses of 122 impacts would provide 10% statistics for these three sample sets.

The above logic was iterated a second time for the extremely large sample sets represented by the impacts on IDE sensors that were located on the East, North and South sides of LDEF. Optical scanning of 3 out of 32 sensors from each of these groups provided estimates of the sample set sizes of 10,000, 4,600 and 4,400 impact sites, respectively. Clearly, the resources were not available to analyze 2,000 samples. However, since the sample sets were so large, it seemed logical to select 10% of the sensors from each location and analyze 10% of the samples on each sensor. This yielded the more practical goal of 200 analyses. Thus, analyses of a total of ~320 impact sites on IDE sensors would provide a first order statistical look at the manmade/natural microparticle population ratio.

To date 79 impact sites on IDE sensors have been analyzed with SEM/EDS and SIMS. Manmade or natural classifications have been assigned to 40 of the residues, or ~ 50%. An extensive background and blank discharge study required to establish the level of contamination and other analytical interferences has been conducted, but more work is required in this area. Although there are significant analytical interferences associated with elemental analyses of impact sites on the ultra high-purity IDE detector surfaces, most of these can be mitigated through recognition. The details and results from the contamination study will be the subject of a future paper.

Impactor Classification

The impactor classifications listed in Table 2 were assigned after reviewing all available data and are subject to the described limitations. Decisions were based on:

1) the element distributions depicted in the two dimensional ion maps described above,

2) the relative (to Si) ion abundance values calculated for each species in the central craters of the impact features, and

3) the local contamination environment in and around the impact feature.

Because the IDE detectors were constructed from silicon and aluminum, these two important elements could not be identified in impactor residues. Thus, aluminum oxide particle residues were undetectable, and the Si in natural impactor residues was also undetectable.

Identification of natural meteoroid residues followed the guidelines of the Meteoroid and Debris SIG. Residues were labeled natural if they had elemental compositions that were similar to common components of chondritic meteorites or interplanetary dust particles (IDP's). Most IDP's of micron size have solar elemental abundance ratios for Mg, Si, Fe, S, Ca, Ni and Na in decreasing order of abundance. The atomic abundances of Mg, Si and Fe are roughly equal in most IDP's and are an order of magnitude more abundant than Ca, Ni and Na. In practice, residues were labeled as natural meteoroids if they had high Mg and Fe abundances and either lacked or contained low abundances of elements not common in primitive meteoritic materials. Relative ion sensitivity factors ,"RSF" (see below) were taken into account when estimating compositions from ion intensity maps.

Manmade particle residues were identified by the presence of relatively high concentrations (>100 ppm in most cases) of metals such as Ti, Zn, Cr, Cu or Ag. Manmade classifications were also assigned to 4 residues (out of the 79) containing only Na, K and Mg under the assumption that these were the remains of impacts with paint particles that used silicate or magnesium oxide pigments. This assumption is subject to change as more insight into possible Na, K and Mg contamination is gained. All 4 of the impacts were located on leading edge sensors.

Indeterminate classifications were assigned to 39 residues that did not fall into either of the above categories. These included sites that contained only traces of Na and/or K. A subset of the indeterminate classification, labeled "clean", was composed of impact sites with no detectable residues. These may be the result of aluminum oxide particle impacts, a likelihood for impacts on the leading (East) and the North and South sides, or the result of impacts from very high velocity submicron interplanetary dust particles that completely vaporize, a statistical likelihood for impacts on the trailing (West) and Space end trays. As the study progresses, some of the indeterminate classifications may change.

Consideration of all the analytical data was complex and subject to interpretation. As a result, some impactor classifications may change as further insight into the analytical contamination and background issues is gained. For example, H, F and Cl were present in all central craters. This has been traced to ppm level contamination from HF and HCl during sensor fabrication. Na, K, and Mg to a lesser extent were present in the majority of impacts and may be from residual background contamination. The presence of these elements is reported since there is no verification of background contamination at this time, and there were many impact sites with little or no detectable Na, K or Mg. The Cameca instrument has been retrofitted with an electron flood gun that will permit depth profile studies of the IDE sensor surfaces through the insulating SiO_2 layer. These depth profiles should reveal the presence of bulk and interfacial contaminants in the SiO_2 and Si.

Depth profiles through the conductive aluminum layer have already shown that this material is contaminated with ~10-100 ppm of Ca. This severely limits the ability to identify Ca in impact sites. Calcium was detected all around the areas surrounding nearly all impact discharges, but was absent from

most central craters, or present at concentrations much lower than the background. The few instances where Ca was found in the impact craters at higher than background levels are reported.

Differential sputtering of the contamination layer from the highly textured impact sites was unavoidable and was considered when interpreting the SIMS data. The phenomenon results from beam shadowing effects caused by the craters, ridges, and even the smaller "hills and valleys " of the vapor deposited Al surface layer. In practice, ion images of control areas in the vicinity of the impacts, both before and after oxygen beam sputter cleaning, provided an estimate of the level of "background" concentrations for these areas. Images of impact areas (after sputter cleaning) were interpreted with these values in mind, and only after all sites on a given sensor were examined.

In order to gain insight into the distribution of the material in the surface contamination layer after an impact induced discharge occurred,a series of "blank discharges" were induced on a flight sensor using an ultrapure Si shard. SIMS analyses of these "blanks" showed that the C, Na, Mg, K, Ca bearing contamination layer was blown away from the central craters and surrounding zone of vaporized Al by the discharge energy. Only Si and Al were detected within the discharge craters and vaporization zones of these analytical blank discharges.

SIMS Data Reduction Method

Besides the obvious visual information, each pixel of the element ion maps contains digitized intensity information that can be reduced to a semi-quantitative number relative to the Si signal. The following steps were employed in this process:

1.) Ion maps were displayed on a computer screen individually and a rectangular box was electronically scribed around the same area of interest on each map.

2.) The cumulative pixel intensity data within the box was summed.

3.) Relative ion sensitivity factors (RSF) for species implanted in Si were used to correct the intensity values (see Table 1, refs. 2 and3).

4.) The corrected ion intensity values were normalized to the Si ion signal recorded for the same area.

5.) Data from individual craters were normalized for the number of pixels summed, the beam intensity during data collection, and the detector conditions during data collection.

Table 1 Relative Sensitivity Factors (RSF's) for species implanted in silicon (ref. 2 and 3). In general the values are applicable for elemental concentrations up to ~1%.

Ion	RSF	Ion	RSF
C^+	0.007	Cu^+	1.61
Na^+	139	Zn^+	0.054
Mg^+	18.0	Ag^+	0.694
Al^+	36.0		
Si^+	1.00	H^-	0.602
K^+	125	C^-	0.161
Ca^+	38.5	F^-	102
Ti^+	13.9	Al^-	0.250
Cr^+	7.69	S^-	5.10
Fe^+	1.85	Cl^-	26.3
Ni^+	1.35	Au^-	0.658

The reduced data have several limitations. First, RSF values for species implanted in Si were not appropriate for species deposited in or on aluminum or for deposits that were massive enough to form their own matrix. They are valid only for elements implanted in Si up to concentrations of ~1%. The assumption that the negative Si electrode exposed in the central crater region of impacts on the IDE sensors acted as an ion trap was the reason for selecting these RSF values. This assumption was based on the knowledge that positive ion pairs act as the charge carriers in the IDE discharge event and would theoretically be implanted in the Si. It should be noted that, in general, the RSF values for species in other matrices follow the same relative trend.

The second major limitation of the semi-quantitative data was the result of an artifact of the Cameca 3f operational protocol. This instrument could only collect data for one mass at a time. Up to ~50Å of material was sputtered away during each ion imaging step. Thus, the data for each element was from a different layer within the residue. For example, several hundred angstroms of material was removed between the imaging of Mg and Fe. This is a significant limitation on the ability to deduce impactor chemical composition from the scant residues.

Examples of semi-quantitatively reduced SIMS data are included in this report. More detailed interpretations will be presented in a future report after analysis of several ground based hypervelocity microparticle impact induced discharge features on retrieved IDE sensors is completed, and a more thorough understanding of contamination issues is gained.

RESULTS AND DISCUSSION

Overview

To date, 79 impacts on IDE sensors have been analyzed with SIMS. These include 36 impacts on two IDE sensors from LDEF tray C-9 (leading, or east side), 18 impacts on four different sensors from tray C-3 (trailing, or west side), 12 impacts on one sensor from tray B-12 (north side), 4 impacts on one sensor from tray D-6 (south side), 6 impacts on one sensor from the earth end tray G-10, and 3 impacts on one sensor from the space end tray H-11. Of the 79 impacts, 57 were formed from particles estimated to have been <3 μm in size, 18 were formed from particles estimated to have been 5-20 μm in size, and 3 were formed from particles estimated to have been 30-50 μm in size.

Microimpactor residue classifications are listed in Table 2. Elements identified at concentrations significantly higher than the background are listed for each impact site. The term "trace" refers to less than 10 ppm concentration, relative to Si, for all elements except Na and K, where the term refers to <100 ppm. Examples of impact feature morphologies, SIMS elemental ion maps, and quantitatively reduced SIMS data are presented in Figs. 1-3.

Minimum crater size of IDE impact features is ~10 μm due to the electrical discharge damage caused when the capacitor sensor was triggered (ref. 1). The sensors responded to hypervelocity particles ~0.5 μm or larger (assumed density of ~3 g/cm^3). Observed spall zone sizes for small particle impacts into the crystalline IDE sensor surfaces were typically ~3X the size of the central craters (Table 2, ref. 1). The central crater size of microimpacts in crystalline materials typically approximate the impactor size (ref. 4). Thus, it was impossible to estimate impactor size in the range of 0.5 to ~3 μm from the crater morphology on active IDE sensors.

The formation mechanism for craters ~10-25 μm in size on active IDE sensors was dominated by the impactor's kinetic energy (KE) transfer, but the discharge energy caused the entire crater and spall area to melt and fuse. "Crater" dimensions listed are for this fused area, but are more representative of spall zone size. Impactor size for these features was estimated to have been ~1/3 of the fused crater/spall size.

Formation of larger impact craters (>30 μm) was totally dominated by the impactor ΔKE and there were frequently shock induced spall zones around the craters. These larger impact sites had the typical morphology of hypervelocity impacts in crystalline material and impactor size was estimated to have been slightly less than the central crater size. The spall sizes listed in Table 2 are for the maximum dimension of the associated spall zones.

Impact identification Nos. in Table 2 refer to the IDE sensor number followed by a crater number (i.e. 1176-C3). Locations of all impacts were recorded for future reference. Craters were not always sequentially numbered since SIMS analyses were not performed on all craters that were labeled for further study in the initial optical scan. This was primarily due to the inability of the SIMS beam to reach every crater on a given surface without venting and reloading the sample in a different orientation, and in no way affected the randomness of the micro-impact site selections.

Considering all of the limitations described above, the impactor classifications cannot be taken as absolute, but there is moderate confidence in their accuracy within the described limitations of the study. Limits can be ascribed to the manmade/natural ratios based on the results to date. ***Future adjustments, resulting from better understandings of contamination issues and impactor residue deposition mechanisms, and from additional analyses of orbital impact sites, may alter the statistical distribution of manmade and natural impactor classifications deduced from currently available data.*** Additionally, the combination of this data set with data from other LDEF investigators should provide a more accurate assessment of the microparticle population ratio in LEO.

Tray C-3 (Trailing [wake], or West side)

There was an average of 10 impacts per sensor on tray C-3. Impactor residues in 18 impact sites on four different sensors were classified as: 5 manmade, 3 natural and 10 indeterminate. Four of the manmade residues had Ti and/or Zn in high concentrations and were assumed to be from paint particles. Two of these particles were <~3 μm in size, and the other two were ~20 and ~40 μm in size. Residue from a fifth manmade impactor (<~3 μm in size) was identified by the presence of significant amounts of Cr along with Mg and Fe.

Figure 1a shows a SEM micrograph of impact No. 1382-C2 from tray C-3 with its 22 μm wide central crater and its 65 μm wide spall zone. SIMS ion maps for Na^+, Mg^+, Si^+, K^+, Ti^+ and Zn^+ are shown in Fig. 1b. The black box in these images outlines the image area that was selected for quantitative data reduction. A bar graph of the calculated concentrations, relative to Si=1.0, is shown in Fig. 1c and provides an example of the type of data that can be evaluated further as the study progresses. It should be possible to derive significant information about the chemical composition of the non-volatile components of many impactors from these types of data after contamination interferences are better understood.

The three natural micrometeorite residues on tray C-3 sensors were all identified by the presence of Mg and Fe. Two of the impacts were made by small (<~3 μm) particles and had Na, Mg, K, Fe and Mg, and Ca, Fe, Ni present in residues. The third impact (No. 1336-C4)had a 23 x28 μm central crater (as described above) with no additional spall zone. A residue containing Na, Mg, K, Ca and Fe was found in the crater. Probable impactor size was estimated to have been ~10 μm. Figure 2a is an optical micrograph of this impact. SIMS ion maps are shown in Fig. 2b, and Fig. 2c shows a bar graph plot of the reduced image data for the central crater region.

Ten of the 18 impact sites had insufficient debris remaining to be positively identified above the background levels. This situation could be the result of natural microimpactors that had very high encounter velocities (>>10 km/s), or impacts from aluminum oxide particles which were not detectable in the Al/Si substrate. Central craters in these impacts ranged in size from 10-25 μm. Figure 3a shows an example of a medium size impact in the "clean" category, No. 1359-C6. Probable impactor size was estimated at ~10 μm. Figures 3b shows some of the ion maps associated with this impact, and Fig. 3c

shows a bar graph of the reduced SIMS data for the central crater. It is anticipated that further analysis of this type of data in "clean" impact sites will lead to quantitation of background contamination levels and allow more accurate assessment of chemical compositions of the non-volatile impactor components.

If all 10 of the "clean" impact sites are assumed to have been caused by small, high speed natural particles, the manmade/natural ratio equals 5/13=0.38. This microparticle value is significantly higher than the assumed ratio of 0.1 for all impactors striking the trailing edge of satellites in low earth orbit (LEO) and could be the result of contamination interferences. However, the IDE data showed that the long term average flux of particles >0.5 μm in size varied drastically during the nearly 6 year long mission (ref. 5). Of the total of 290 impacts on these sensors, 186, or 64% occurred during the first year. The overall mission flux rate measured by the sensors matched that measured by other investigators (ref. 6). It is possible that orbital debris impacts caused the enhanced rate during the first year. (This topic is discussed in more detail in ref. 5.) The chemical analysis data collected thus far, subject to the stated limitations, seem to support this scenario.

Tray C-9 (Leading [ram], or East side)

There was an average of 311 impacts/sensor on tray C-9. Using the same criteria described above, impactor residues in 36 impact sites on 2 different sensors were classified as: 11 manmade, 5 natural and 20 indeterminate. If 19 of the 20 "indeterminate" impactors (those that were "clean" or had only Na and K present in the craters) are assumed to have been Al_2O_3 particles, then the manmade/natural ratio would equal 30/5=6.0. This micorparticle ratio is somewhat lower than the assumed ratio of 10 for all impactors on the leading edge of satellites in LEO, but considering the limitations of the current study, this preliminary result is reasonable. It should be noted that the long term impact flux measured by these leading edge sensors did not vary substantially and matched the flux rates measured by other LDEF investigators (ref. 6).

Of the 11 manmade impactors, 9 were particles that were <~3 μm in size and 2 were particles estimated to have been 30-40 μm in size. Of the 9 small particle residues, one had only Ti and a trace of Na and K, three residues contained Cu in addition to Na, K and Mg, one contained Cu along with Na, K, Mg, Fe and traces of Ti and Cr, and four residues contained only Na, K and Mg.

The two largest manmade debris impacts examined have significant amounts of impactor residue. Residue from an ~30 μm particle contained Na, Mg, Ti, Cr, Fe, Cu, Zn and Ag and could be from a small piece of electrical component with paint. Residue from a 40 μm particle contained high concentrations of H, C, Ti, Cr and Fe and could have been a piece of painted plastic or a paint particle with an organic binder. (This was the only high concentration H, C residue found in the 79 impact sites.)

All 5 of the natural impactors were identified by the presence of Mg and Fe. Only one residue had Ca above background. One particle was estimated to have been <~3μm in size, and the other 4 were estimated to have been ~5-10 μm in size.

Of the 20 "indeterminate" impactors, 16 were <~3 μm in size, and 4 were ~4-8 μm in size. This could support the assumption that most of these impactors were small aluminum oxide spheres (from solid rocket motor exhaust). Zinner, et al., have reported that 8 out of 11 small particle impact craters examined on Ge capture cells from LDEF tray E-8 (near leading edge) contained only Al and O residues (ref. 7).

Tray D-6 (South side)

There was an average of 137 impacts/sensor on tray D-6. Impactor residues in 4 craters examined on one sensor were classified as : 1 manmade (Na, K, Mg, Cu) and 3 indeterminate. All craters were

formed by particles <~3 μm in size. These results are too preliminary to draw any conclusion other than the obvious, expected result that orbital debris did strike the North side of the satellite. Cu was the indicator for the manmade impactor residue. Al_2O_3 particles, or small high speed natural particles could have caused the other impacts.

Tray B-12 (North side)

There was an average of 143 impacts/sensor on tray B-12. Impactor residues in 12 craters examined on one sensor were classified as: 4 manmade, 6 natural and 2 indeterminate (clean). Natural impactors were all identified by the presence of Mg and Fe. Only one of these had significant Ca. Three of the 6 natural impactors were <~3 μm in size, and three were ~5 μm in size. The two indeterminate impactors were both <~3 μm in size.

Three of the 4 manmade impactors were <~3 μm in size and the fourth was ~6 μm in size. Residue from the largest impactor contained Fe, Cu and Zn along with Na, K, and Mg. One of the 3 smaller impacts contained Na, Mg, K and traces of Cu and Ag, one contained Na, Mg, K, Ti and Zn, and one contained Na, Mg, Fe and Cu.

Tray G-10 (Earth end)

There was an average of 10 impacts/sensor on tray G-10. Two out of 6 small particle(<~3 μm) impactor residues analyzed on one sensor were classified as manmade based on the presence of Fe and Ti in one and Ti and Cr in the other. The other four impactors were classified as indeterminate since only traces of Na and K were found in the craters.The only conclusion that can be drawn from these data is the expected result that orbital debris did strike the Earth end of the satellite. It is interesting to note that the entire impact set on the Earth end sensors was formed by particles <4 μm in size. (The sensors were shielded from highly oblique (<4°) grazing impacts.)

Tray H-11 (Space end)

There was an average of 21 impacts/sensor on tray H-11. Three impacts on one sensor were analyzed and classified as: 2 manmade and 1 natural. The natural impactor, estimated to have been ~8 μm in size, left a residue containing Na, Mg, K, Ca and Fe. Only Ti and Zn were detected in the residue from one small manmade particle (<~3 μm). The second manmade particle, estimated to have been ~6 μm in size, also left a residue containing Ti and Zn, but traces of Na and K were detected in the crater. Both particles were probably pieces of paint. No conclusions can be drawn from this small sample set on the Space end tray, but the early results indicate that there may have been more orbital debris strikes on the Space end than expected.

Comments

The presence of Cu in 5 of the 11 manmade impactor residues on sensors from the East panel, and 4 of the 5 manmade impactor residues found on sensors from the North and South sides of LDEF, is unexpected. This may be due to higher than normal, heterogeneously distributed background levels of Cu, or some other unidentified mass interferent. However, a review of all residue compositions shows that Cu was only detected in impact sites on the East, North and South sides of the satellite. The IDE impact record shows that the LDEF passed through several orbital debris clouds during its first year in

orbit that affected only these three sides of the spacecraft. Thus, it is possible that Cu bearing debris may be a significant component of these debris clouds. If the Cu is shown not to be a contaminant in future work, this could point to a specific source type for this debris. The other manmade impactors were presumably paint particles as discussed above.

Remaining resources for this study will be utilized for the following tasks:

1) continued analysis and interpretation of data collected to date in order to further define the nonvolatile chemical composition of impactors,

2) continued contamination studies including depth profiles down to the Si substrate that will address background contamination levels for Na, Mg, K and Cu.

3) EDS and Auger spectroscopic studies of heavy deposits of impactor residues and surface contamination features in order to determine the composition and possible cross interference of these species

4) analyses of several simulated (Fe hypervelocity particles) impact sites on an active flight sensor, and

5) analysis of as many flight impact sites as possible until the optimum number of 320 is reached.

SUMMARY

To date, 79 impacts on IDE sensors have been analyzed with SIMS. These include 36 impacts on two IDE sensors from LDEF tray C-9 (leading, or east side), 18 impacts on four different sensors from tray C-3 (trailing, or west side), 12 impacts on one sensor from tray B-12 (north side), 4 impacts on one sensor from tray D-6 (south side), 6 impacts on one sensor from the earth end tray G-10, and 3 impacts on one sensor from the space end tray H-11. Of the 79 impacts, 57 were formed from particles estimated to have been <3 μm in size, 18 were formed from particles estimated to have been 5-20 μm in size, and 3 were formed from particles estimated to have been 30-50 μm in size. Residue from manmade debris, mostly paint particles and metal bits, has been identified in craters on all trays. (Aluminum oxide particle residues were not detectable on the Al/Si substrates.)

Preliminary estimates of the manmade/natural microimpactor population ratio for the East and the West sides of LDEF were calculated assuming that unknown impactor residues were all manmade or all natural, respectively. The calculated ratios were 6.0 for the East and 0.38 for the West. These values are subject to change as more information on contamination interferences, and more analyses impact sites is collected. Additionally, the combination of this data set with data from other LDEF investigators should provide a more accurate assessment of the microparticle population ratio in LEO.

Quantitative analyses of impactor residue chemical composition is underway, but results will not be reported until a better understanding of contamination issues is gained.

Cu was detected in 9 out of 16 "manmade" impacts on sensors from the East, North and South sides of LDEF, but was not detected in any of the 9 "manmade" impacts on sensors from the West, Space and Earth ends of the satellite. If, after further investigation, the Cu is shown not to be a contaminant, this could point to a specific source type for this debris.

The results to date are generally consistent with the IDE impact record which showed highly variable long term microparticle impact flux rates on the West, Space and Earth sides of the LDEF which could not be ascribed to astronomical variability of micrometeorite density. The IDE record also showed episodic bursts of microparticle impacts on the East, North and South sides of the satellite, denoting passage through orbital debris clouds or rings.

REFERENCES

1. C.G. Simon, J.L.Hunter, D.P. Griffis and J.J. Wortman, "Ion Microprobe Elemental Analyses of Impact Features on Interplanetary Dust Experiment Sensor Surfaces", NASA CP 3134, pp. 529-548 (1991).

2. R.G. Wilson, F.A. Stevie and C.W. Magee, Secondary Ion Mass Spectrometry - A Practical Handbook for Depth Profiling and Bulk Impurity Analysis, J. Wiley & Sons, p. E-17 (1989).

3. Ibid, p. E-22.

4. B.G. Cour-Palais, "The Current Micrometeoroid Flux at the Moon for Masses $\leq 10^{-7}$ g from the Apollo Window Surveyor 3 TV Camera Results", Geochimica et Cosmochemica Acta, Vol. 3, pp. 2451-2462 (1974).

5. C.G. Simon, J.D. Mulholland, J.P. Oliver, W.J. Cooke and P.C. Kassel, "Long-Term Microparticle Flux Variability Indicated by Comparison of Interplanetary Dust Experiment (IDE) Timed Impacts for LDEF's First Year in Orbit with Impact Data for the Entire 5.77 year Orbital Lifetime",

6. C.G. Simon, J.C. Mandeville, J.A.M. McDonnell, M. Mirtich and R.W. Walker, "M&DSIG Microcrater Committee Report", in NASA CP-3194, (1993).

7. S. Amari, J. Foote, C. Simon, P. Swan, R. Walker and E. Zinner, "SIMS Chemical Analysis of Extended Impacs on the Leading and Trailing Edges of LDEF Experiment AO187-2", in NASA CP-3194, (1993).

Table 2. Microparticle residue classifications for 79 impacts on IDE sensor surfaces based on SIMS analyses. (See text for explanation of crater and spall zone sizes.) *Na not looked for in all sites.

Impact No.	Size (μm) Crater	Spall	Elements Detected with SIMS	Impactor Classificaton manmade	natural	indeterminate
LDEF Tray C-3 (Trailing [wake], or West side)						
1300-C1	36x54	138	(Na, Mg, K, Ca)--(Ti, Fe)	X		
1300-C2	13x18	-	clean (trace Na)			X
1300-C3	12	-	Na, Mg, K, Fe		X	
1300-C4	13	-	clean			X
1300-C5	11	-	Na, K, Mg, Cr, Fe	X		
1300-C6	10	-	clean			X
1300-C7	12	-	Na, K, Ti	X		
1300-C8	12	-	Na, Mg, K, Ti	X		
1336-C1	10	-	clean (trace Na)			X
1336-C4	23x28	-	Na, Mg, K, Ca, Fe		X	
1359-C4	10	-	clean			X
1359-C5	9x12	-	clean (trace Na, Mg)			X
1359-C6	18x25	42	clean			X
1359-C7	12	-	clean			X
1382-C2	22	65	Na, Mg, K, Ti, Zn	X		
1382-C4	9	-	(trace Mg, Ca, Fe, Ni)		X	
1382-C5	10	-	clean			X
1382-C9	15x20	-	clean (trace Mg)			X
LDEF Tray C-9 (Leading [ram], or East side)						
1176-C1	23	-	Na, Mg, K, Fe		X	
1176-C2	9	-	clean (trace Na, K)			X
1176-C3	9	-	Na, K			X
1176-C4	11	-	Na, K, Cu	X		
1176-C5	32	212	Na, Mg, Ti, Cr, Fe, Cu, Zn, Ag	X		
1176-C6	23x37	-	Na, K			X
1176-C7	50	138	H, C, Ti, Cr, Fe	X		
1176-C8	9	-	Na, Mg, K	X		
1176-C9	12x16	-	Na, Mg, K--(Fe)			X
1176-C10	9	-	Na, Mg, K, Cu	X		
1176-C11	9	-	Na, K			X
1176-C12	10	-	Na, Mg, K	X		
1176-C13	9	-	Na, Mg, K, Cu	X		
1176-C14	9	-	Na, K			X
1176-C15	9	-	Na, K			X
1176-C16	10	-	Na, K			X
1176-C17	11	-	Na, Mg, K, Fe, Cu (trace Ti, Cr)	X		
1176-C18	22x25	-	Na, Mg, K, Fe		X	
1176-C19	11	-	Na, Mg, K	X		
1176-C20	11	-	Na, Mg, K	X		
1293-C1	13x17	-	*clean			X
1293-C2	24x31	-	*Mg, K, Fe		X	
1293-C3	18	-	*Mg, K, Ca, Fe		X	
1293-C4	12	-	*Mg, Fe		X	

Table 2. [continued] Microparticle residue classifications for 79 impacts on IDE sensor surfaces based on SIMS analyses. (See text for explanation of crater and spall zone sizes.) *Na not looked for in all sites.

Impact No.	Size (μm) Crater	Spall	Elements Detected with SIMS	Impactor Classificaton manmade	natural	indeterminate
LDEF Tray C-9 (Leading [ram], or East side) {continued}						
1293-C5	22x28	-	*clean			X
1293-C7	12	-	*clean			X
1293-C8	10	-	*clean			X
1293-C12	12	-	Ti (trace Na, K)	X		
1293-C13	9	-	clean			X
1293-C14	9	-	clean			X
1293-C15	11	-	clean			X
1293-C16	11	-	clean			X
1293-C17	9	-	clean			X
1293-C18	11	-	clean			X
1293-C19	13	-	clean			X
1293-C20	11	-	clean			X
LDEF Tray D-6 (South side)						
1252-C3	10x13	-	Na, Mg, K, Cu	X		
1252-C4	10	-	clean (trace K)			X
1252-C5	10	-	clean (trace K)			X
1252-C9	10	-	clean (trace K)			X
LDEF Tray B-12 (North side)						
1298-C1	11x19	34	Na, Mg, K, Fe		X	
1298-C2	10	-	clean			X
1298-C6	15x20	38	Na, Mg, K, Fe		X	
1298-C7	10	-	Na, Mg, K, Ca, Fe		X	
1298-C8	16x20	30	Na, Mg, K, Fe, Cu, Zn	X		
1298-C9	15	-	Mg, Fe		X	
1298-C10a	10	-	Na, Mg, K (trace Cu, Ag)	X		
1298-C10b	10	-	Na, Mg, K, Ti, Zn	X		
1298-C11	11	-	clean			X
1298-C12	9x13	-	Na, Mg, Fe		X	
1298-C13	10	-	Na, Mg, Fe		X	
1298-C14	10	-	Na, Mg, Fe, Cu	X		
LDEF Tray G-10 (Earth end)						
1172-C5	9	-	Na, Mg,Ti,Fe	X		
1172-C6	9	-	clean (trace Na, K)			X
1172-C7	11	-	Na, K			X
1172-C8	10	-	clean (trace Na, K)			X
1172-C10	9	-	clean (trace Na, K)			X
1172-C11	10	-	Na, K, Ti, Cr	X		
LDEF Tray H-11 (Space end)						
1255-C1	20	32	Ti, Zn (trace Na, Mg)	X		
1255-C2	23x27	-	Na, Mg, K, Ca, Fe		X	
1255-C4	11	-	Ti, Zn	X		

(A)

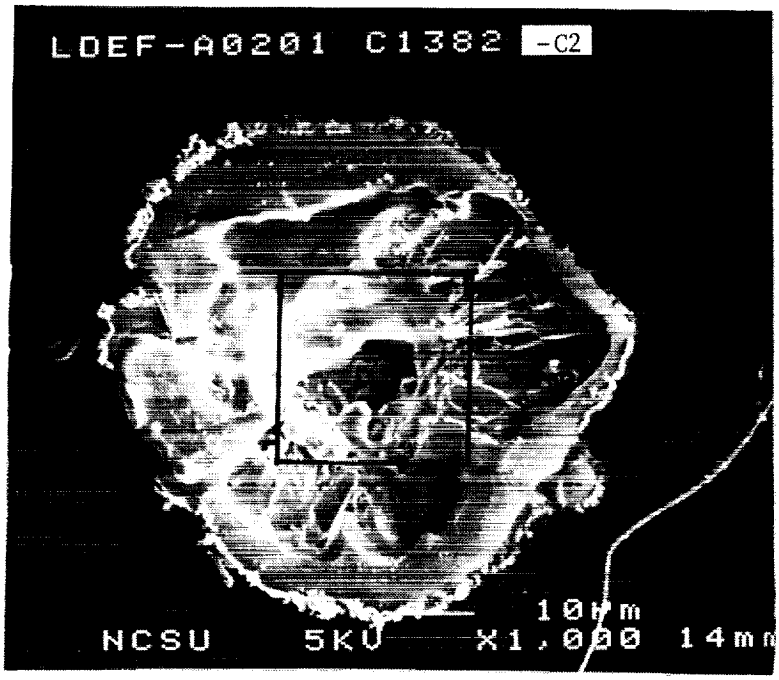

(C)

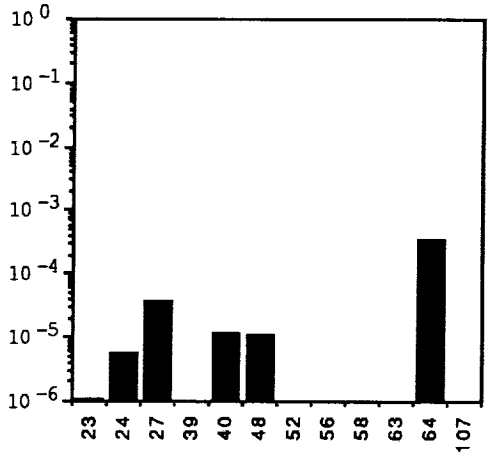

(B)

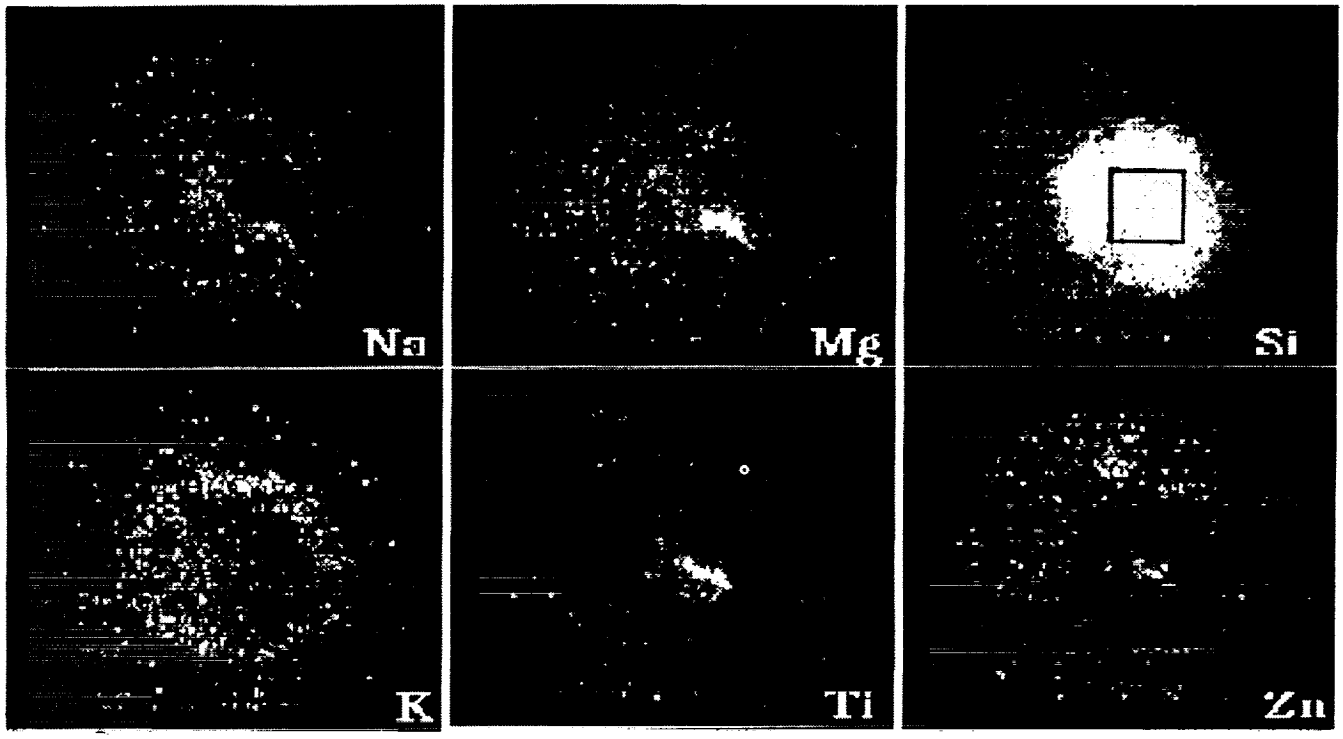

Figure 1. Example of a manmade debris impact (1382-C2) on an IDE sensor mounted on LDEF tray C-3 (Trailing or West side). (A) SEM micrograph. (B) Secondary positive ion images of impact area. Imaged area is 150 μm in diameter. Intensities are uncorrected for relative ion yields. Note exposed area of Si and SiO_2 defined by the Si^+ map. (C) Bar graph plot of corrected ion intensity data for boxed area.

(A)

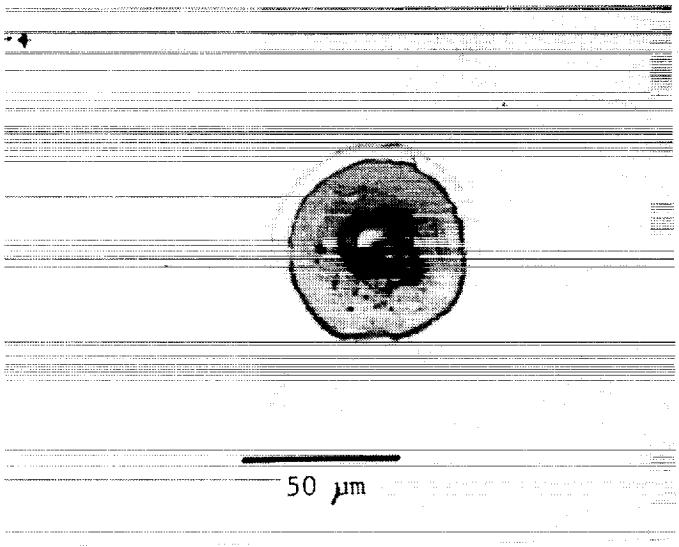

(C)

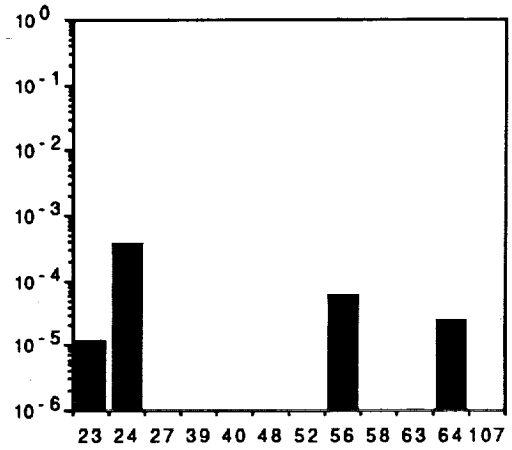

(B)

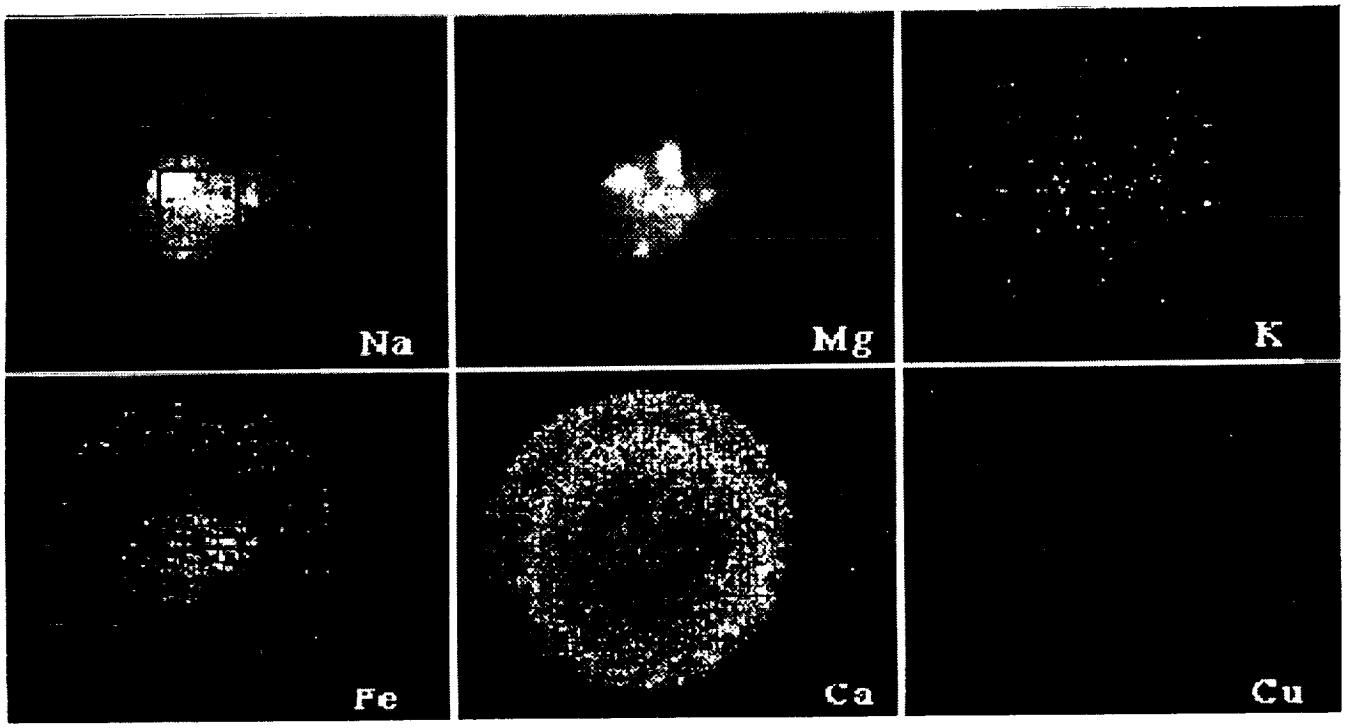

Figure 2. Example of a natural micrometeorite impact (1336-C4) on an IDE sensor mounted on LDEF tray C-3 (Trailing or West side). (A) Optical micrograph. (B) Secondary positive ion images of impact area. Imaged area is 150 μm in diameter. Intensities are uncorrected for relative ion yields. (C) Bar graph plot of corrected ion intensity data for boxed area. Note the low intensity for mass 64 (Cu+) in the ion image and the relatively high concentration value displayed in the bar graph. This methodological artifact raises the minimum detectable Cu level to the 100 ppm range. The high Ca+ background intensity surrounding the impact has been traced to contamination in the top layer of aluminum on the substrate.

(A)

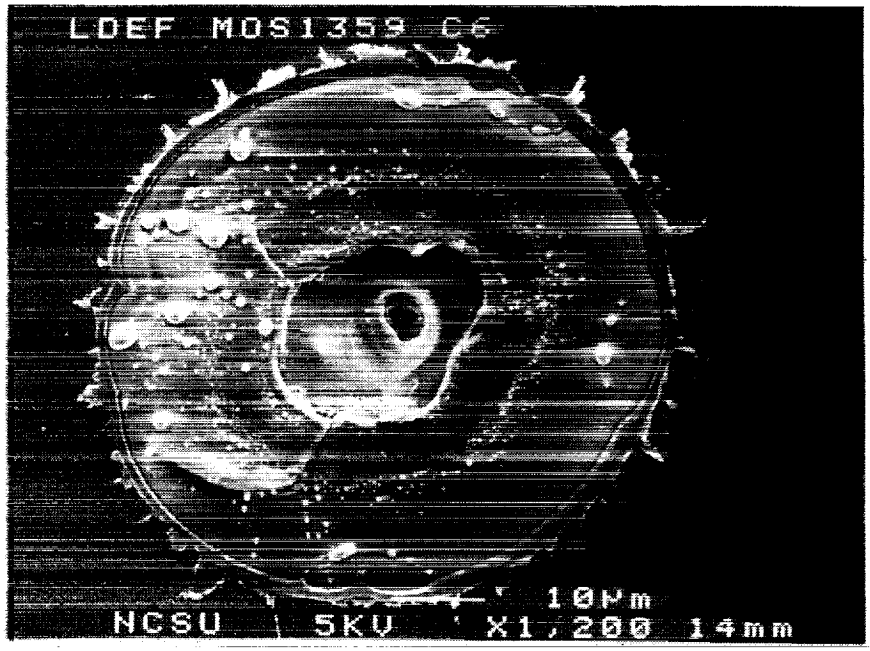

(B)

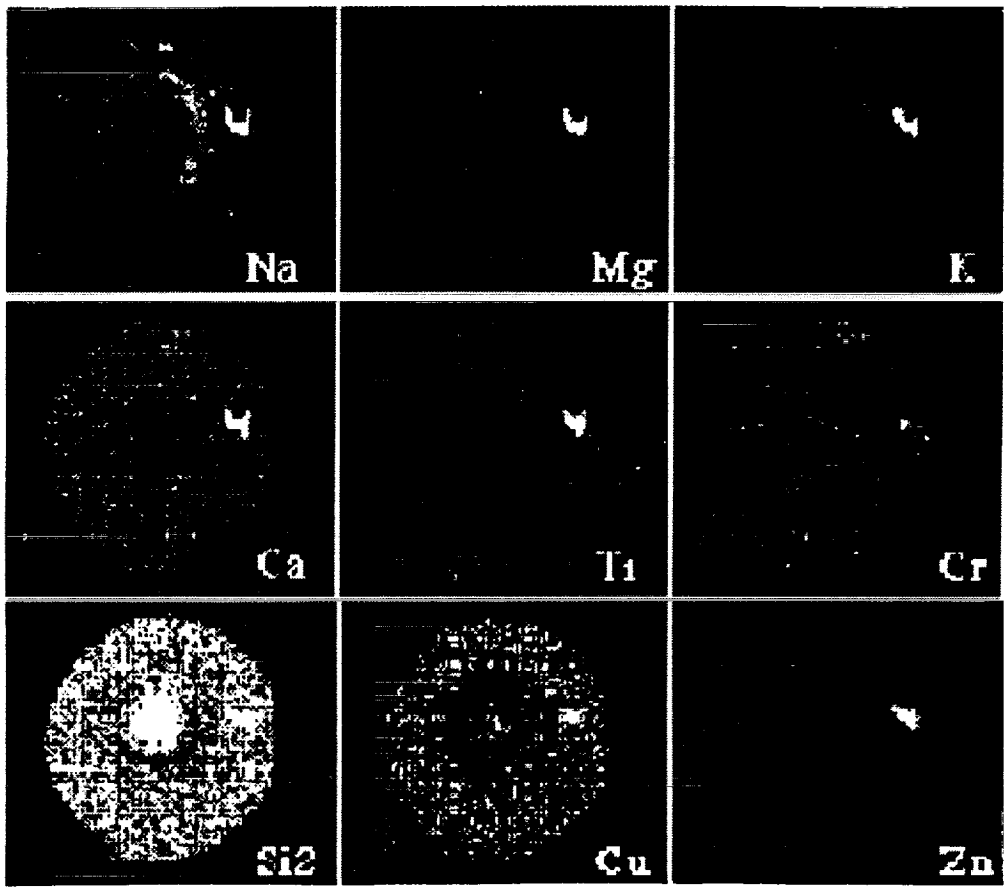

Figure 3. Example of an indeterminate impact (1359-C6) on an IDE sensor mounted on LDEF tray C-3 (Trailing or West side). (A) SEM micrograph. (B) Secondary positive ion images of impact area. Imaged area is 150 µm in diameter. Intensities are uncorrected for relative ion yields. Note central crater area defined by the Si_2^+ map. Bright spot of Na, Mg, K, Ca, Ti, Zn is a contaminate well outside of the impact crater.